



Published in final edited form as:

Arterioscler Thromb Vasc Biol. 2024 January ; 44(1): 143–155. doi:10.1161/ATVBAHA.123.319909.

FAM222A, part of the BET-regulated basal endothelial transcriptome, is a novel determinant of endothelial biology and angiogenesis

Aspasia Tzani^{1,3}, Stefan Haemmig^{1,3}, Henry S. Cheng^{1,3}, Daniel Perez-Cremades^{1,3}, Marina Augusto Heuschkel^{1,3}, Anurag Jamaiyar^{1,3}, Sasha Singh^{1,3}, Masanori Aikawa^{1,3}, Paul Yu^{1,3}, Tianxi Wang^{2,3}, Sun Ye^{2,3}, Mark W. Feinberg^{1,3}, Jorge Plutzky^{*,1,3}

¹Division of Cardiovascular Medicine, Brigham and Women's Hospital, Boston, MA 02115

²Department of Ophthalmology, Boston Children's Hospital, Boston, MA 02115

³Harvard Medical School, Boston, MA 02115

Abstract

Background: Bromodomain and extra-terminal domain-containing epigenetic reader proteins (BETs), including BRD4, orchestrate transcriptional programs induced by pathogenic stimuli, as intensively studied in cardiovascular disease and elsewhere. In endothelial cells (ECs), BRD4 directs induced pro-inflammatory, pro-atherosclerotic transcriptional responses; BET inhibitors, like JQ1, repress these effects and decrease atherosclerosis. While BET effects in pathogenic conditions has prompted therapeutic BET inhibitor development, BET action under basal conditions, including ECs, has remained understudied. To understand BET action in basal endothelial transcriptional programs, we first analyzed EC RNA-Seq data in the absence versus presence of JQ1 before using BET regulation to identify novel determinants of EC biology and function.

Methods: RNA-Seq datasets of human umbilical vein ECs without and with JQ1 treatment were analyzed. After identifying C12orf34, also known as Family with Sequence Similarity 222 Member A (FAM222A), as a previously unreported, basally expressed, potentially JQ1-induced EC gene, FAM222A was studied in endothelial and angiogenic responses *in vitro* using siRNA silencing and lentiviral overexpression, *in vitro*, *ex vivo* and *in vivo*, including aortic sprouting, Matrigel plug assays and murine neonatal oxygen-induced retinopathy (OIR).

***Correspondence to:** Jorge Plutzky, MD, Cardiovascular Medicine, Brigham and Women's Hospital, Harvard Medical School, 77 Ave. Louis Pasteur NRB742, Boston, MA 02115. jplutzky@bwh.harvard.edu.

Author Contributions

A.T. and J.P. conceived the hypothesis and coordinated the project. A.T., S.H., H.S.C., D.P.C., S.S., M.E., M.H., A.J., P.Y., T.W., S.Y., M.W.F. and J.P. contributed to experimental design and data analysis. A.T. performed *in vitro* mechanistic studies, animal studies, bioinformatic analysis and con-focal imaging experiments. A.T. and S.H. performed plasmid cloning and lentivirus production. T.W. and S.Y. performed murine retinal studies. A.T. and J.P. wrote the manuscript.

Disclosures

None

Supplemental Material

Expanded Materials & Methods

Tables S1-S4

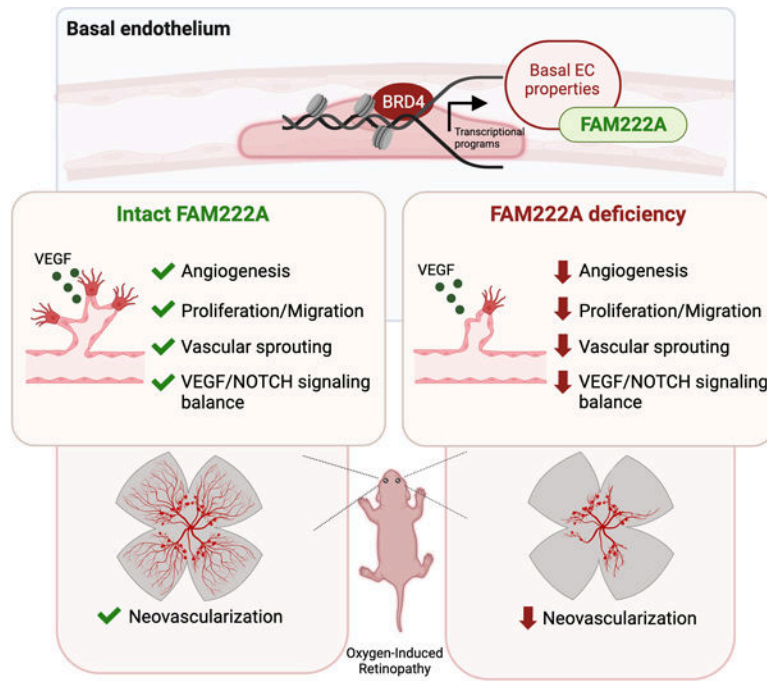
Figures S1-S4

Major Resources Table

Results: Resting EC RNA-Seq data indicates BETs direct transcriptional programs underlying core endothelial properties including migration, proliferation and angiogenesis. BET inhibition in resting ECs also significantly induced a subset of mRNAs, including FAM222A - a unique BRD4-regulated gene with no reported EC role. Silencing endothelial FAM222A significantly decreased cellular proliferation, migration, network formation, aorta sprouting and Matrigel plug vascularization through coordinated modulation of VEGF and NOTCH mediator expression *in vitro*, *ex vivo*, or *in vivo*; lentiviral FAM222A overexpression had opposite effects. *In vivo*, siFAM222A significantly repressed retinal neovascularization in neonatal murine oxygen-induced retinopathy through similar angiogenic signaling modulation.

Conclusions: BET control over the basal endothelial transcriptome includes FAM222A, a novel, BRD4-regulated, key determinant of endothelial biology and angiogenesis.

Graphical Abstract



Keywords

bromodomain-containing epigenetic reader proteins; BETs; BRD4; endothelial cells; endothelium; FAM222A; angiogenesis; VEGF; NOTCH; oxygen-induced retinopathy

Introduction

The bromodomain and extra-terminal domain-containing protein family (BETs), including BRD2, BRD3 and BRD4, are epigenetic reader proteins that orchestrate specific transcriptional programs involved in differentiation, identity, and induced cell state transitions, as implicated in cancer, atherosclerosis, myocardial hypertrophy and pulmonary hypertension.¹ BETs control gene expression by binding to specific acetylated lysine residues on chromatin histone tails, thus enabling assembly of transcriptional machinery

assembly, including RNA Polymerase II (Pol II).^{2,3} BET control over pathogenic transcription has prompted pursuit of BET inhibitors as therapeutic agents, including in cardiovascular disease.¹ In the endothelium, cytokine stimulation induces BRD4-regulated inflammatory and pro-atherosclerotic gene expression; BET inhibitors repress these same responses *in vitro* and *in vivo*, as reported by us and others.^{2,4,5} Despite a focus on BETs in pathologic transcriptional programs, BETs also modulate basal gene expression, as seen with TNF α stimulation of endothelial cells (ECs) causing loss of BRD4-dependent transcription of specific genes expressed under basal conditions.^{1,2} Although largely unstudied, BET action in basal transcription is an important component of BET biology in physiologic versus pathologic conditions as well as the potential therapeutic BET inhibitor effects.⁶

Initially, we sought to define the basal BET-regulated endothelial transcriptome, analyzing RNA-Seq data in human umbilical vein ECs before and after exposure to the well-validated, highly specific pan-BET inhibitor JQ1. In addition to using JQ1 as a tool to probe BET action in ECs under basal conditions, we also reasoned since BET regulate induced, canonical pro-inflammatory and pro-atherosclerotic endothelial genes, BETs might similarly control important genes under basal conditions, providing an orthogonal approach to identifying novel determinants of EC function.

Interrogation and gene ontology (GO) analysis of basal HUVEC RNA-Seq data when BET activity was intact (no JQ1) vs inhibited (with JQ1) established BETs govern key endothelial transcriptional programs, including angiogenesis. This data also underscored another understudied aspect of BET transcriptional action, namely genes whose expression was induced, not repressed, after BET inhibition. Further consideration of basally expressed endothelial mRNAs most induced after BET inhibition and with unknown function pointed to Chromosome 12 Open Reading Frame 34 (C12orf34), also known as Family with Sequence Similarity 222 Member A (FAM222A). Subsequent data presented here establish FAM222A is abundantly expressed in ECs and essential for EC proliferation, migration, and angiogenesis by modulating VEGF and NOTCH mediator expression. *In vivo*, FAM222A silencing repressed retinal neovascularization in the neonatal murine oxygen-induced retinopathy (OIR), a well-established angiogenesis model of retinopathy of prematurity (ROP).^{7,8} Taken together, this data expands insight into BET control over endothelial transcription and identifies FAM222A as a key novel determinant of endothelial biology and angiogenesis.

Methods

Detailed experimental methods and a Major Resources Table are available in the Supplemental Material. Additional methods used in experimental methods, data analysis and the materials used to conduct this research are also available from the corresponding author.

Ethical Approval

Institutional approval was obtained for all mouse studies, as performed in C57Bl/6J mice (Jackson Laboratories), maintained in a pathogen-free facility with standard light/dark

cycling and ad libitum food [containing 20% protein, 4.5% fat, PicoLab Rodent Diet20 , #5053, DietLabs) and water access (Animal protocol #2016N000115, Harvard Medical School Institutional Animal Care and Use Committee).

Human Specimen

Frozen sections were prepared from human healthy male carotid arteries that were obtained from the Division of Cardiovascular Medicine, Brigham and Women's Hospital, in accordance with the institutional review board-approved protocol for use of discarded human tissues (protocol number: 2010-P-001930/2).

Data Sharing

Our published basal HUVEC RNA-seq and ChIP-seq datasets with or without JQ1 (500nM, 3 hours) are available (accession numbers GSE53999 and GSE539998)².

Cell transfection

HUVEC were transfected with small interference RNAs (siRNAs, Sigma; sequences in Table S1) for FAM222A, BRD2, BRD3, BRD4, EGR1 or Scrambled Control overnight using RNAi Max (13778075, Invitrogen, MA, USA) as described in the manufacturer's protocol. The FAM222A siRNA #2 was a SMARTpool siRNA (L-015010-02-0005, Dharmacon). bEND.3 cells were transfected with siRNAs for FAM222A or Control overnight using Lipofectamine 2000 (11668019, Invitrogen, MA, USA) as above. All siRNAs used for transfection at 50 nM.

Expression plasmids, Lentivirus production and HUVEC transduction

For FAM222A overexpression studies in HUVEC, the cDNA of full length FAM222A was cloned into the lentiviral EGFP vector pULTRA (24129, Addgene) by digestion of the restriction enzyme EcoRI. Lentiviral vectors were produced by triple transient transfection of HEK 293T cells with a packaging plasmid psPAX2 (12260, Addgene), a plasmid encoding the envelope of vesicular stomatitis virus (VSVg) (pMD.2G) (12259, Addgene) and the pULTRA plasmid encoding FAM222A or GFP using Lipofectamine 3000 per manufacturer's protocol. Viruses were collected 48 and 72 hours after transfection, titered and incubated with HUVEC for 16 hours in presence of 8 µg/ml polybrene (TR-1003-G, Sigma) at a range of multiplicity of infection (MOI). The virus- transducing medium was replaced with fresh EGM-2 medium after infection. The transfection efficiency was monitored by GFP expression.

In vitro functional assays

Scratch wound assay: Cell migration was assessed by scratch wound assay using Culture-Insert 2 Well 35mm µ-Dishes (Ibidi, 501149017). HUVEC transfected with FAM222A or control siRNAs or transduced with FAM222A or Control lentiviral particles were cultured for 48 hours in 12-well plates and re plated at 21,000 cells per well into the µ-Dishes. Inserts were lifted at 60 hours after transfection, and cells were imaged using an Eclipse TE2000-U inverted microscope (Nikon) at 2× and 4× over time to assess for wound closure. When indicated, HUVEC were treated with VEGF, Mitomycin C or DAPT following

overnight serum starvation. BrdU proliferation assay: Cell proliferation was measured using the BrdU Cell Proliferation ELISA kit as described by the manufacturer (Abcam). *Matrigel tube formation assay*: Network tube formation was assessed by the Endothelial Cell Tube Formation Assay (Corning). Briefly, Matrigel basement membrane matrix was added to 24-well culture plates and incubated at 37°C until gelation occurred. Matrigel was not supplemented with additional growth factors. HUVEC transfected with FAM222A, or Control siRNAs were cultured for 48 hours and reseeded at 120,000 cells/well. Network tube formation was assessed at 16 hours post plating by labeling the cells with Calcein AM fluorescent dye and quantitated by counting the number of tubes formed per high-power field. *Spheroid assay*: To assess endothelial sprouting, HUVEC were transfected or transduced as above and after 48 hours were cultured overnight in hanging drops on nonadherent plastic dishes in EBM-2 medium with 0.2% methylcellulose (Sigma-Aldrich) using 1,000 cells/spheroid. Spheroids were embedded in a collagen matrix and incubated for 24 hours in the presence of VEGF. Number of sprouts and total sprout length of 10 spheroids per condition were used for data analysis by using NIH ImageJ software. *Apoptosis assay*: Cell apoptosis was measured using the ApoLive-Glo Multiplex assay as described by the manufacturer (Promega). *Viability assay*: Cell viability was assessed by the Cell counting kit (WST-8) as indicated by the manufacturer (Abcam). *Annexin V/Propidium Iodide (PI) Assay*: Early and late apoptosis was assessed in siRNA transfected HUVEC in the presence or absence of Staurosporine (4hrs) using the Dead Cell Apoptosis Kit with Annexin V Alexa Fluor™ 488 & PI as described by the manufacturer (Invitrogen). Specimens were examined by flow cytometry using the BD LSR II Flow Cytometer (BD Biosciences, San Jose, CA, USA), and the data were analyzed with the FlowJo v9 software (BD Biosciences).

Animal Studies

Studies were performed in C57Bl/6J mice (Jackson Laboratories), maintained in a pathogen-free facility with standard light/dark cycling and ad libitum access to food [containing 20% protein and 4.5% fat, PicoLab Rodent Diet20, #5053, DietLabs) and water. All animal procedures conform to the “Guide for the Care and Use of Laboratory Animals” published by the US National Institutes of Health (NIH publication No. 85–23, revised 1996). Animal protocol approval (#2016N000115) was granted by the Harvard Medical School Institutional Animal Care and Use Committee (IACUC).

Aortic ring assay

Aortic ring assay was performed as previously described by us and others with minor modifications.^{9–12} Briefly, aortas were harvested from 6–8 weeks old C57Bl/6J mice, cut into 1 mm pieces, and placed in 12-well plates with 1ml serum reduced EGM-2 medium. Aortas were then transfected with FAM222A or Control siRNAs diluted in Opti-MEM using Lipofectamine 2000 transfection reagent (Invitrogen) or infected with FAM222A or Control Lentiviral particles overnight. The following day, the rings were embedded into 100 ul of growth-factor reduced Matrigel (Corning) and incubated for 10–15 minutes at 37 °C to allow Matrigel polymerization. The embedded rings were then carefully fed with endothelial growth medium EGM2. The medium was changed every 2 days. Microvessel sprouting was observed at 10 days post embedding and quantified using Image J software (NIH).

Aortic ring assay was additionally performed by embedding the transfected/infected rings in 150 μ l of matrix containing Rat-tail Collagen Type I (Gibco, A1048301), media 199 10 \times phenol red free (ThermoFisher), 140 mM NaHCO₃ (Sigma), 1 M NaO (Sigma) and autoclaved water as previously described¹³. Phase-contrast imaging of the sprouted rings was performed at day 8 post embedding and quantification of the sprouting area was measured using Image J software (NIH).

Matrigel plug in vivo assay

HUVEC transfected with FAM222A or Control siRNAs or infected with FAM222A or Control Lentiviral particles were cultured for 24 hours before admixed with high concentration Matrigel basement matrix (Corning, 1,000,000 cells/ml). As previously described^{14,15} 500 μ l of Matrigel admixed with transfected or transduced HUVEC were injected subcutaneously into the flank area of 6–8 weeks old C57Bl/6J mice and allowed to solidify. The plugs were collected 7 days post implantation and the surrounding granulation tissue was removed. The color of the plugs ranged from a (light) yellow (to a pink depending on the amount of blood vessel ingrowth). Angiogenesis in plugs was analyzed by measuring their Hemoglobin content using the Drabkin method (Sigma).

Oxygen-induced retinopathy (OIR) model

OIR was induced as previously described^{16,17}. Briefly, pups (129S) of both sexes along with their nursing mother were exposed to 75% oxygen from postnatal day 7 to 12. At postnatal day 12, they were returned to room air and siRNAs were injected intravitreally at 12 as previously published¹⁸. Approximately, 0.5 μ l of solution containing FAM222A siRNA (2 μ g/eye) was injected into the vitreous body of the right eye of anesthetized neonates with 1.5% isoflurane. The left eye was injected with an equal volume of Control siRNA and used as vehicle control. Intravitreal injections were accomplished by careful insertion of a 35-gauge needle attached to a Hamilton syringe under a surgical microscope. At postnatal day 17 the mice were anesthetized; eyes were enucleated and fixed and both retinas were dissected and collected for PCR assay or whole-mount analysis. The retinas were whole-mount stained with antibodies against CD31 (1:30, Cat#: 550274, BD Pharmingen), Alexa Fluor 594-labeled isolectinB4 (*Griffonia simplicifolia*) (1:200, Cat#: I21413, Thermo Fisher), to visualize ECs and FAM222A (1:200, Cat#: PA5-59093, Thermo Fisher). Cell nuclei were stained with 4',6-diamidino-2-phenylindole (DAPI, 0.5 μ g/ml, Cat#: 4083, Cell Signaling). Retinas were imaged using a Zeiss AxioObserver.Z1 microscope and AxioCam MRm camera. Avascular and neovascularization areas were quantified as percentage of whole retinal area using a fully automated deep learning segmentation method¹⁹.

Statistical analysis

Data are shown as mean \pm SEM unless otherwise noted. Unpaired Student's t test was used for single comparisons. One-way ANOVA followed by Tukey post-hoc test was used to determine the significance of one independent variable between more than two groups. Comparisons between two groups and two nominal variables were performed using Two-way ANOVA followed by Tukey post-hoc test. Differences were considered statistically significant at $p < 0.05$. Statistical analysis was performed using GraphPad Prism.

Results

BETs regulate the EC transcriptome under basal conditions, including FAM222A, an essential determinant of EC proliferation and migration

To investigate BET endothelial action under basal conditions, we analyzed existing RNA-Seq datasets (GSE53999)^{2,20} in human umbilical vein ECs (ECs, here and throughout) under standard maintenance conditions and without or with BET inhibitor JQ1 treatment (500 nM²), identifying basally expressed genes (RPKM>1) whose mRNA levels were significantly altered by BET inhibition. BETs significantly regulated mRNA expression of EC genes under basal conditions, with JQ1 repressing a significant cassette of EC genes while also significantly increasing mRNA levels of another distinct subset of basally expressed genes (Figure 1A). To better understand these BET-dependent, divergent EC transcriptional programs, we analyzed those mRNAs repressed or induced significantly (log 2-fold mRNA change) by JQ1 [3 hrs treatment (false discovery rate, FDR, <0.01), Figure 1B, Upper Panel]. In GO pathway analyses (Figure 1B, Lower Panel), basally expressed EC gene transcripts significantly repressed by JQ1 were predominantly involved in functional EC properties of cell adhesion, cell cycling and apoptosis (Figure 1B, blue-shaded). A smaller but significant subgroup of basally expressed EC genes manifest significant mRNA induction after JQ1 treatment, with GO analysis indicating predominate regulation of angiogenesis, including major angiogenic signaling pathways like NOTCH (Figure 1B, red-shaded).

BET inhibition increasing gene expression, a form of *trans* induction, has remained largely understudied and poorly understood, despite its relevance to BET action and potential responses to therapeutic BET inhibitors.^{1,4,21} As such, we further investigated basally expressed EC genes significantly induced by JQ1. Given the prior GO data (Figure 1C), this basal EC RNA-Seq dataset of JQ1-induced genes was analyzed for non-structural proteins without known involvement in cellular proliferation, migration or EC biology. Among the nine most JQ1-induced EC genes, GADD45B and TENT5C have reported roles in cellular proliferation and proliferation^{22,23}, H2BC5 is a histone protein²⁴, while five other genes - HEXIM1, ID2, FOS, VIP, and C9 - have reported EC effects, including vascular morphogenesis (Figure 1C).²⁵⁻²⁹ Of note, most of these JQ1-induced genes, specifically GADD45B, TENT5C, HEXIM1, ID2 and FOS are reported as involved in NOTCH signaling, in keeping with the GO analysis.^{22,30-34} The open reading frame protein C12orf34, also known as FAM222A, emerged as the sole gene significantly expressed in ECs under basal conditions, potently induced by JQ1, and lacking a known role in migration, proliferation or EC biology, prompting our further study of this novel gene consisting of a 1,359 base pair coding region, 3 exons, 452 amino acids, and no obvious predicted domains or protein family association. (Figure S1)

In line with RNA-Seq data, FAM222A mRNA expression increased in a dose-dependent manner in ECs after BET inhibition with JQ1 or the structurally distinct BET inhibitor I-BET (Figure S2A). JQ1 also increased activity of a human FAM222A promoter luciferase reporter in a dose-dependent manner after EC transfection (Figure S2B) and FAM222A protein levels, as evident in immunofluorescent EC staining, which was

primarily nuclear (Figure S2C). Before further investigating FAM222A, we sought evidence for FAM222A's potential relevance in human tissue. Immunohistochemistry staining demonstrated FAM222A protein in the endothelial layer of human carotid artery specimens (Figure 1D, Upper Panel; Figure S2D), as also seen in mouse aorta (Figure S2E). FAM222A expression was restricted predominantly to ECs as compared to other vascular and inflammatory cell types, including primary human coronary artery smooth muscle cells (SMCs), fibroblasts, and monocyte-derived macrophages (Figure 1D, Lower Panel). Given this data, we moved on to investigate BET regulation of FAM222A, testing if BRD2, BRD3 and/or BRD4 explained the increased FAM222A mRNA expression by the pan-BET inhibitor JQ1, using specific, validated small interference RNA (siRNAs) to each BET isoform (Figure S2F). Only siBRD4, and not siBRD2 or siBRD3, significantly decreased FAM222A mRNA levels (Figure 1E), as seen under both basal conditions and after JQ1 exposure (Figure S2G).

In line with BRD4 acting through chromatin binding, analysis of our existing Chromatin Immunoprecipitation (ChIP) sequencing datasets in ECs indicated BRD4 binds to the FAM222A promoter regulatory regions at two distinct sites in either the absence or presence of JQ1 while JQ1 treatment increased RNA Pol II recruitment to these same FAM222A promoter locations (Figure S2H). Given BRD4 binding on the FAM222A promoter either with or without JQ1, we hypothesized additional transcriptional regulators act in cooperation with BRD4 to direct FAM222A expression. By overlapping data of EC genes significantly induced by JQ1 treatment ($\log_2fc > 1$) with transcription mediators predicted to bind to the FAM222A promoter (ChIP Atlas, ± 10 kb from TSS³⁵), early growth response (EGR)-1 was identified as the sole gene with both JQ1 induction and predicted FAM222A promoter binding (Figure 1F, Venn diagram). Subsequent *in silico* analysis demonstrated two distinct EGR1 binding sites on the FAM222A promoter region.^{36,37} Indeed, JQ1 treatment increased significantly both mRNA and protein levels of EGR1, an established pro-angiogenic mediator³⁸ (Figure 1F, lower left). Moreover, overexpression of EGR1 increased FAM222A promoter activity in transfected ECs under basal conditions and after JQ1 treatment (Figure 1F, lower right) while repressing EGR1 expression with a validated siRNA (Figure S2I) significantly decreased JQ1's effects on FAM222A expression, which declined further after siBRD4 transfection (Figure 1G).

Having identified FAM222A as an EGR1-regulated gene basally expressed in ECs and further induced after BET inhibition as well as GO predicted action, we next investigated FAM222A in key functional EC responses involving growth, proliferation, and migration, with and without pro-angiogenic stimuli of VEGF and hypoxia. Both VEGF stimulation (50 ng/ml, 3 hrs) and hypoxia (1% O₂, 3 hrs) significantly induced FAM222A mRNA expression in ECs (Figure 1H) while the cytokines TNF α , TGF β 2, and IL1 β had no effect on basal FAM222A expression (Figure S2J). These VEGF and hypoxia effects on FAM222A mRNA did not further increase JQ1-stimulated induction of FAM222A mRNA (data not shown), as also the case with concomitant JQ1 and TNF α , TGF β 2 or IL1 β (Figure S2J).

We next assessed EC growth in the presence or absence of specific, validated FAM222A siRNA (90% decrease in FAM222A mRNA and protein, Figure S3A). siFAM222A

significantly decreased EC growth vs siControl-transfected cells (siCtl, Figure 1I), without increasing apoptosis, as seen in caspase 3/7 (Figure 1J) and Annexin V/staurosporine treatment assays (Figure S3B). Silencing FAM222A decreased EC proliferation significantly in BrdU incorporation assays under both basal and VEGF-stimulated conditions (vs siCtl, Figure 1K). siFAM222A also decreased VEGF-induced proliferation in synchronized ECs, which was independent of contact-inhibition (Figure S3C). In scratch wound assays, siFAM222A decreased EC migration and wound closure significantly under both basal (–38%) and VEGF-stimulated conditions (–48%, both vs siCtl, Figure 1L, middle and right, respectively). Next, to test if siFAM222A decreased wound closure by impairing EC proliferation or migration, scratch assays were repeated in mitotically-inactive, mitomycin C-treated ECs, which did not alter siFAM222A-mediated decreased wound closure (–46% vs siCtl, Figure S3D). siFAM222A-treated ECs did manifest a modest but significant decrease in cell viability (WST-8 assays, Figure S3E), in keeping with the significant decrease in proliferative and migratory capacity seen after FAM222A silencing.

To further test FAM222A involvement in EC proliferation and migration, we undertook gain-of-function experiments using Green fluorescent protein (GFP) -Lentiviral FAM222A overexpression, which increased FAM222A mRNA (380-fold) and protein (6-fold) significantly (Figure S3F). FAM222A-overexpressing ECs had significantly increased proliferation in a multiplicity of infection (MOI)-dependent manner (Figure 1M) and wound closure rates (Figure 1N, middle and right). Thus, in both loss- and gain-of function studies, FAM222A was found to significantly effect EC proliferation and migration under basal and VEGF stimulated conditions.

FAM222A regulates angiogenic responses *in vitro*, *ex vivo* and *in vivo* through coordinated modulation of VEGF and NOTCH pathways

Given FAM222A involvement in VEGF-stimulated EC responses, we further explored FAM222A in network formation and vascular sprouting as key angiogenic responses.^{11,39} Silencing FAM222A decreased EC capillary-like tube formation (Matrigel assays) under both basal (47%) and VEGF-stimulated (52%) conditions (Figure 2A). siFAM222A also decreased VEGF-induced vessel sprout length (–82%) and sprout number (–80%) in EC spheroids (Figure 2B). FAM222A overexpression had the opposite effects on EC sprouting, with LentiFAM222A-infected ECs forming more (+ 117% sprout number) and longer (+ 54% sprout length) vascular sprouts (Figure 2C and S3G), with distinct changes on “tip-like” EC appearance vs non-infected ECs.

Although Matrigel as a medium for investigating angiogenesis *in vitro* has some potential limitations,^{11,14} we used this approach to connect with our prior data and experience in two other models of angiogenesis, namely an *ex vivo* aortic ring^{9,10,12} sprouting angiogenesis model and in *in vivo* Matrigel plugs.¹⁵ We first compared the effect of FAM222A silencing vs overexpression on sprouting of murine Matrigel-embedded aortic rings. In keeping with effects seen *in vitro*, siFAM222A treatment decreased aortic ring microvessel formation (–76%, Figure 2D) significantly while FAM222A overexpression had the opposite effects (+191%, Figure 2E). Similar results were seen after repeating FAM222A silencing or overexpression in sprout assays performed in collagen (Figure S3H and S3I). We next tested

if ECs with FAM222A silencing (siFAM222A) or overexpression (LentiFAM222A) or respective controls, when mixed with Matrigel prior to flank injection into wild-type mice, altered vessel plug in-growth (Day 7).¹⁵ siFAM222A-treated EC/Matrigel demonstrated significantly decreased vessel growth into Matrigel plugs, as measured using hemoglobin (Hb) content (−55%, Figure 2F, vs siControls). In contrast, FAM222A overexpressing EC/Matrigel plugs had increased vascularization (vs LentiCtl ECs, +29, Figure 2G).

These findings for FAM222A in EC proliferation, migration and vascularization prompted the question of FAM222A involvement in angiogenic signaling pathways. VEGF promotes angiogenesis via carefully coordinated signaling pathways involving multiple proteins, including activating phosphorylation of the VEGF receptor 2 (VEGFR2) and key distal mediators of mitogen-activated protein kinase/extracellular-signal-regulated kinase-1/2 (Erk1/2) and phosphatidylinositol 3-kinase (PI3-K)/Akt.⁴⁰ Given FAM222A's nuclear localization, we investigated if FAM222A controlled expression of VEGF-induced mediators involved in EC proliferation, sprouting, and survival. Indeed, FAM222A silencing decreased mRNA levels of VEGF, the VEGF co-receptor NRP1, the pro-angiogenic growth factor ANG1, its agonist TIE2, and the angiogenic transcriptional factors EGR1 and TAL1 (Figure 2H), all of which are implicated in VEGF-directed EC responses.^{36,41} Concurrently, siFAM222A also increased expression of ANG2 (Figure 2H), a known anti-angiogenic mediator that opposes TIE2-ANG1 effects.⁴² Moreover, the distal VEGF-induced Erk1,2 signaling proteins, including MAPK3 (Erk1), MAPK8 and MAPK14 were also decreased in siFAM222A-treated ECs (Figure 2H). Interestingly, siFAM222A increased VEGFR2 mRNA levels (Figure 2H) while expression of PI3K/Akt pathway genes were unchanged (data not shown). These changes suggested FAM222A controlled expression of these distal VEGF mediators would alter VEGF signaling, which we studied next.

After siFAM222A transfection in ECs (48 hrs), the expected VEGF-induced phosphorylation of VEGFR2, Erk1/2 and Akt were all significantly suppressed (−86%, −56%, −25%, respectively, vs siCtl; Figure 2I and S4A). While siFAM222A did not alter Erk1/2 and Akt protein levels, basal Erk1/2 and Akt phosphorylation were marginally decreased by siFAM222A (Time 0, Figure 2I). Consistent with the mRNA findings, basal VEGFR2 protein levels were also increased by siFAM222A (Figure 2I), suggesting a potential compensatory response to impaired VEGF signaling after loss of FAM222A. To further test FAM222A involvement VEGF signaling, we next investigated VEGF-induced angiogenic responses after FAM222A overexpression in ECs, using our previously validated lentiviral constructs (Figure S3F). VEGF stimulation of FAM222A overexpressing ECs resulted in angiogenic responses that were the opposite of those seen after FAM222A silencing, with increased activating phosphorylation of VEGFR2, Akt, and Erk1/2 (Figure 2J), without altering basal expression of these same proteins (Figure S4B).

VEGF stimulation also activates NOTCH signaling, which offsets angiogenic responses.^{43,44} Given FAM222A's coordinated modulation of multiple angiogenic mediators, we next considered if this extended to the NOTCH pathway. Silencing FAM222A in ECs promoted NOTCH-mediated signals that limit angiogenesis, increasing mRNA levels of NOTCH receptors NOTCH2 and NOTCH4 and the NOTCH ligands Jagged 1 (JAG1) and Delta-like 4 (DLL4) (Figure 2K, left). NOTCH receptors NOTCH1, NOTCH2 and NOTCH4

were all found to be activated, as indicated by increased levels of their intracellular domains (ICD), which depends on NOTCH cleavage by γ -secretase,²⁶ and decreased levels of their transmembrane subunits (NTM; Figure 2K, left). NOTCH-ICD also increases the anti-angiogenic mediators HES1 and HES2,^{45,46} whose mRNA and protein levels were also increased by siFAM222A (Figure 2K). In keeping with siFAM222A increasing NOTCH signaling, repeating these experiments in the presence of the γ -secretase-specific NOTCH inhibitor DAPT [N-[N-(3,5-Difluorophenacetyl)-L-alanyl]-S-phenylglycine t-butyl ester] reversed the siFAM222A effects on all NOTCH signaling mediator mRNAs other than JAG1 (Figure S4C), doing so without altering FAM222A expression (Figure S4D). Functionally, DAPT treatment significantly rescued decreases in EC migration and wound closure after siFAM222A treatment (Figure S4E). Together these findings identify FAM222A as determining endothelial proliferation, migration and angiogenic responses *in vitro* through its coordinated modulation of angiogenic mediators involved in VEGF and NOTCH pathways.

Given that no validated FAM222A-deficient mouse currently exists, we tested the effects of FAM222A deficiency on angiogenesis *in vivo* using siFAM222A in the neonatal oxygen-induced retinopathy (OIR) model, given its extensive validation, representation of both physiologic and pathologic angiogenesis, and accepted replication of retinopathy of prematurity (ROP) in human newborns.⁷ In OIR, postnatal day 7 (P7) mouse pups, and their nursing mothers, undergo hyperoxia (75% O₂) exposure for 5 days (P7-P12), which causes retinal capillary depletion, before being returned to room air (P12-P17), which induces pathologic neovascularization (schematic, Figure 2M), as used by us and others.^{11,17,47,48} After first confirming siFAM222A decreased FAM222A expression in mouse brain ECs (bEND.3), murine EC proliferation and migration (Figure S4F), and FAM222A protein levels in mouse retinal ECs (Figure S4G), intra-vitreous siFAM222A or siCtrl injections in OIR were performed (P12) before initiating the vascular proliferation phase (P12-P17), followed by retinal harvesting (P17). Retinas from siFAM222A-treated pups exhibited significantly reduced vaso-oblivation and neovascularization vs siCtrl-treated mice (P17, Figure 2M). In keeping with *in vitro* findings, siFAM222A intravitreal injection also significantly decreased retinal VEGF mRNA levels while increasing gene expression of the angiogenic repressor HES2 (Figure S4H). Taken together, the data presented here demonstrate BETs regulate the basal endothelial transcriptome, which includes BRD4 control over FAM222A, a previously unreported protein essential for endothelial biology and function that exerts coordinated effects on proliferation, migration, and angiogenesis, as evident *in vitro*, *ex vivo* and *in vivo*.

Discussion

The endothelium's key role in both homeostasis and pathogenesis involves dynamic modulation of endothelial transcriptional programs. BET epigenetic reader proteins help direct these coordinated changes in gene expression by facilitating transcriptional complex assembly, as reported in pathogenic, stimulated EC responses in multiple cardio-pulmonary conditions.^{2,5,49} Here, we used RNA-Seq datasets in the absence or presence of BET inhibition to investigate the largely unexplored issue of BET-dependent transcription in ECs under basal conditions. This transcriptome data revealed BET transcriptional regulation

of genes involved in core aspects of basal EC function, including angiogenesis as well as distinct basally expressed endothelial genes induced after BET inhibition. Further analysis of these basally expressed, JQ1-induced EC mRNAs led to identification of FAM222A as a unique, novel, BRD4-regulated determinant of EC biology and angiogenesis. FAM222A knockdown suppressed VEGF-stimulated EC migration, proliferation and sprouting while FAM222A overexpression had the opposite effects. - responses mediated by coordinated transcriptional modulation of key VEGF and NOTCH pathway mediators. *In vivo*, silencing FAM222A disrupted retinal revascularization in the OIR model by modulating expression of these same proteins involved in controlling angiogenesis. In addition to providing new insight into dynamic BET action in the endothelium, these studies establish FAM222A as a novel, essential determinant of EC biology and angiogenesis.

BETs have received considerable attention although primarily for their role directing induced, pathologic transcriptional programs,^{1,2} like in myocardial pressure overload⁵⁰ and atherosclerosis, including TNF α -induced endothelial NF κ B activation.² Importantly, when these stimuli induce BRD4-mediated transcription, it comes with concomitant loss of BRD4 activity directing gene expression under basal, pre-stimulus conditions.⁵¹ Although largely overlooked, this BRD4-regulated, basal transcriptional program is integral to understanding BET biology, including potential clinical effects of BET inhibitors under study in atherosclerosis, pulmonary hypertension, cancer, inflammatory conditions, and other diseases.^{5,52–56} Prior studies of BET involvement in angiogenesis reflects the complexity of these issues, including differences between stimulated and quiescent endothelium as well as different BET inhibitors. While some reports suggest BET inhibitors decrease angiogenesis, as studied primarily in cancer⁵⁷, others find BET inhibition restores angiogenic responses, as seen with apabetalone⁵⁸, with different distal mediators invoked in the responses seen, mostly under stimulated not resting conditions.

Here, studying EC RNA-Seq data under basal conditions with and without the BET inhibitor JQ1, BETs are shown to control important functional endothelial properties of cell adhesion, migration, and angiogenesis, as seen in GO analyses of basally expressed genes repressed by JQ1 exposure (Figure 1A, 1B). This data also highlighted mRNAs significantly induced by BET inhibition, as seen here with BET inhibitors and siBRD4, responses predicted to also occur through poorly understood endogenous mechanisms that regulate BRD4 activity. Given BET control over canonical, pro-inflammatory, pro-atherosclerotic mediators induced by specific stimuli, we hypothesized similar BET regulation of basal endothelial biology also occurs, which would also provide an orthogonal approach to identifying novel determinants of EC function. This proved to be the case; analysis and annotation of basally expressed, non-structural, JQ1-induced genes with no reported roles in ECs, migration or proliferation pointed to FAM222A, also known as C12orf34 (Figure 1C). Subsequent studies presented here establish FAM222A as basally and predominately expressed in ECs, with mRNA and protein levels potentially increased by BET inhibition involving BRD4 as well as EGR1 (Figure 1D–G).

Cell proliferation and migration are integral to angiogenesis.^{59,60} Pro-angiogenic stimuli, like VEGF and hypoxia, increased FAM222A mRNA and protein levels while silencing FAM222A decreased VEGF-induced EC migration, proliferation, vascular spouting *in*

vitro, *ex vivo* and in Matrigel plug revascularization *in vivo* (Figure 1H–N, 2A–G); FAM222A overexpression had opposite effects. FAM222A silencing did not alter activation of p53 or p53-mediated p21 (data not shown) nor induce apoptosis, excluding these as explanations for decreased cell proliferation and migration after FAM222A silencing. FAM222A deficiency (48 hours) causes transcriptional modulation of players in VEGF and NOTCH pathways underlying angiogenesis. While VEGF drives EC spatial guidance, sprout initiation, and stalk-cell proliferation, NOTCH counters these responses, decreasing EC activity and inducing repressive stalk cell features, including increases in NOTCH-dependent angiogenic repressors HES1, HES2, and HEY^{243,61,62}. siFAM222A modulates expression of all these mediators - decreasing pro-angiogenic targets and growth factors like VEGF, ANG1 and TIE2 while increasing angiogenic repressors. Such coordinated control implicates FAM222A as a key proximal determinant of angiogenic transcriptional programs. Transcriptional responses to FAM222A silencing also disrupts VEGF-induced phosphorylation, decreasing pro-mitogenic MAPK signaling while increasing anti-angiogenic NOTCH effects.⁴⁶ The pharmacologic NOTCH cleavage inhibitor DAPT blocked siFAM222A effects on NOTCH target gene expression and partially reversed siFAM222A-mediated decreased EC migration, suggesting that aberrant NOTCH hyperactivation, a reported cause of decreased EC proliferation,^{60,63} may also contribute to FAM222A's effects on angiogenesis. The only siFAM222A-induced alteration not aligned with decreased angiogenesis was an increase in VEGFR2 levels, which might represent a compensatory response, assuming these changes align with VEGFR2 activity, as requires further study.

In vivo, silencing FAM222A decreased angiogenesis in the neonatal OIR angiogenesis model, with changes that replicate *in vitro* responses. OIR replicates retinopathy of prematurity (ROP) in newborns, with initial vaso-obliteration followed by ischemia/hypoxia-induced neovascularization.^{7,47} Silencing FAM222A during OIR decreased retinal revascularization and VEGF expression while increasing angiogenic repressor HES2 mRNA levels, thus altering EC proliferation and migration during OIR's second, neovascularization phase. Given *in vitro* evidence that FAM222A overexpression promotes angiogenesis, increased FAM222A levels may promote disorders characterized by excess angiogenesis, like ROP, other proliferative retinopathies, and vascular tumors, as warrants further consideration. FAM222A involvement in other angiogenesis models, like hind limb ischemia, and conditions like peripheral arterial disease (PAD)⁶⁴, as also warrants investigation, as prompted by these findings.

In support of our using BET regulation/BRD4 localization in ECs as a strategy for identifying novel determinants of EC biology, only one prior FAM222A-focused report exists, which suggested FAM222A expression is restricted to neurons and might promote Alzheimer's Disease (AD).⁶⁵ The data provided here clearly extends FAM222A action beyond the central nervous system (CNS) and establishes its involvement in non-pathologic processes. At the same time, our data also raises questions if FAM222A in brain ECs might be involved in these reported CNS effects. Of note, in support of FAM222A involvement outside the CNS, its induction after BET inhibition, and its cardiovascular relevance, FAM222A is among the mRNAs most induced in the myocardium of BET inhibitor-treated mice undergoing transaortic constriction.⁵⁰ Whether this FAM222A signal derives from

myocardial ECs or cardiomyocytes, which contain less FAM222A than ECs (data not shown), is unclear but also requires investigation.

Taken together, we establish here BET control over dynamic endothelial gene expression involves basal transcriptional programs. Using basal BET regulation and BRD4 action for endothelial gene discovery enabled identification of FAM222A, which is demonstrated to be a novel, key determinant of endothelial cell migration, proliferation, and angiogenesis *in vitro*, *ex vivo* and *in vivo*.

Supplementary Material

Refer to Web version on PubMed Central for supplementary material.

Acknowledgments

The authors would like to thank Hong Wang for her valuable assistance with animal studies and *in vitro* techniques.

Sources of Funding

A.T. was supported by the George and Marie Vergottis Foundation (Postdoctoral Fellowship, Harvard Medical School) and the Cashman Family Foundation; Y.S. was supported by the NIH/NEI (R01EY030140, R01EY029238) and the BrightFocus Foundation. J.P. was supported by NHLBI R56 HL125894 and the Arbour Way Foundation.

Non-standard abbreviations and acronyms

| | |
|-------------------------------|---|
| FAM222A | Family with sequence similarity 222 member A |
| BETs | Bromodomain and extra-terminal domain-containing epigenetic reader proteins |
| C12orf34 | Chromosome 12 Open Reading Frame 34 |
| EC | Endothelial cell |
| HUVEC | Human umbilical vein endothelial cell |
| TNFα | Tumor necrosis factor alpha |
| VEGF | Vascular endothelial growth factor |
| OIR | Oxygen-induced retinopathy |
| ROP | Retinopathy of prematurity |
| GADD45B | Growth arrest and DNA damage inducible beta |
| TENT5C | Terminal nucleotidyltransferase 5C |
| H2BC5 | H2B clustered histone 5 |
| HEXIM1 | HEXIM P-TEFb complex subunit 1 |
| ID2 | Inhibitor of DNA binding 2 |

| | |
|------------------|---|
| FOS | Fos Proto-Oncogene, AP-1 transcription factor subunit |
| VIP | Vasoactive intestinal peptide |
| C9 | Complement C9 |
| EGR1 | Early Growth Response 1 |
| SMC | Smooth muscle cell |
| CD31 | Cluster of differentiation 31 |
| GFP | Green fluorescent protein |
| MOI | Multiplicity of infection |
| VEGFR | Vascular endothelial growth factor receptor |
| Erk1/2 | Extracellular signal-regulated kinase 1/2 |
| PI3-K/Akt | Phosphatidylinositol 3-kinase/Akt |
| NRP1 | Neuropilin 1 |
| ANG1 | Angiopoietin 1 |
| ANG2 | Angiopoietin 2 |
| TIE1 | Tyrosine kinase with immunoglobulin like and EGF like domains 1 |
| TIE2 | Tyrosine kinase with immunoglobulin-like loops and epidermal growth factor homology domains-2 |
| TAL1 | TAL BHLH transcription factor 1 |
| MAPK3 | Mitogen-activated protein kinase 3 |
| MAPK8 | Mitogen-activated protein kinase 8 |
| MAPK14 | Mitogen-activated protein kinase 14 |
| ICD | Intracellular domain |
| NTM | NOTCH transmembrane subunit |
| DAPT | N-[N-(3,5-Difluorophenacetyl)-L-alanyl]-S-phenylglycine t-butyl ester |
| HES1 | Hes family BHLH transcription factor 1 |
| HES2 | Hes family BHLH transcription factor 2 |
| HEY2 | Hes related family BHLH ratnscription factor with YRPW motif 2 |
| DLL4 | Delta-like 4 |
| HEK | Human embryonic kidney |

References

1. Borck PC, Guo LW, Plutzky J. BET Epigenetic Reader Proteins in Cardiovascular Transcriptional Programs. *Circ Res* 2020;126(9):1190–1208. [PubMed: 32324495]
2. Brown JD, Lin CY, Duan Q, et al. NF-kappaB directs dynamic super enhancer formation in inflammation and atherogenesis. *Mol Cell* 2014;56(2):219–231. [PubMed: 25263595]
3. Wu T, Kamikawa YF, Donohoe ME. Brd4's Bromodomains Mediate Histone H3 Acetylation and Chromatin Remodeling in Pluripotent Cells through P300 and Brg1. *Cell Rep* 2018;25(7):1756–1771. [PubMed: 30428346]
4. Tsujikawa LM, Fu L, Das S, et al. Apabetalone (RVX-208) reduces vascular inflammation in vitro and in CVD patients by a BET-dependent epigenetic mechanism. *Clin Epigenetics* 2019;11(1):102. [PubMed: 31300040]
5. Zhang M, Wang B, Urabe G, et al. The BD2 domain of BRD4 is a determinant in EndoMT and vein graft neointima formation. *Cell Signal* 2019;61:20–29. [PubMed: 31075399]
6. Slaughter MJ, Shanle EK, Khan A, et al. HDAC inhibition results in widespread alteration of the histone acetylation landscape and BRD4 targeting to gene bodies. *Cell Rep* 2021;34(3).
7. Stahl A, Connor KM, Sapielha P, et al. The mouse retina as an angiogenesis model. *Invest Ophthalmol Vis Sci* 2010;51(6):2813–2826. [PubMed: 20484600]
8. Smith LE, Wesolowski E, McLellan A, et al. Oxygen-induced retinopathy in the mouse. *Invest Ophthalmol Vis Sci* 1994;35(1):101–111. [PubMed: 7507904]
9. Icli B, Wara AKM, Moslehi J, et al. MicroRNA-26a Regulates Pathological and Physiological Angiogenesis by Targeting BMP/SMAD1 Signaling. *Circ Res* 2013;113(11):1231–1241. [PubMed: 24047927]
10. Baker M, Robinson SD, Lechertier T, et al. Use of the mouse aortic ring assay to study angiogenesis. *Nat Protoc* 2012;7(1):89–104.
11. Nowak-Sliwinska P, Alitalo K, Allen E, et al. Consensus guidelines for the use and interpretation of angiogenesis assays. *Angiogenesis* 2018;21(3):425–532. [PubMed: 29766399]
12. Bellacen K, Lewis EC. Aortic ring assay. *Journal of Visualized Experiments* 2009;(33).
13. Kapoor A, Chen CG, Iozzo RV. A simplified aortic ring assay: A useful ex vivo method to assess biochemical and functional parameters of angiogenesis. *Matrix Biol Plus* 2020;6–7.
14. Vignetti D, Theocharis AD. The Extracellular Matrix Methods and Protocols Methods in Molecular Biology 1952.
15. Target Discovery and Validation Reviews and Protocols Volume 1, Emerging Strategies for Targets and Biomarker Discovery
16. Sun Y, Liu CH, SanGiovanni JP, et al. Nuclear receptor ROR α regulates pathologic retinal angiogenesis by modulating SOCS3-dependent inflammation. *Proc Natl Acad Sci U S A* 2015;112(33):10401–10406. [PubMed: 26243880]
17. Sun Y, Ju M, Lin Z, et al. SOCS3 in retinal neurons and glial cells suppresses VEGF signaling to prevent pathological neovascular growth. *Sci Signal* 2015;8(395):ra94. [PubMed: 26396267]
18. Taniguchi T, Ichi Endo K, Tanioka H, et al. Novel use of a chemically modified siRNA for robust and sustainable in vivo gene silencing in the retina. *Sci Rep* 2020;10(1):22343. [PubMed: 33339841]
19. Xiao S, Bucher F, Wu Y, et al. Fully automated, deep learning segmentation of oxygen-induced retinopathy images. *JCI Insight* 2017;2(24).
20. Giacinti C, Giordano A. RB and cell cycle progression. *Oncogene* 2006;25(38):5220–5227. [PubMed: 16936740]
21. Ray KK, Nicholls SJ, Ginsberg HD, et al. Effect of selective BET protein inhibitor apabetalone on cardiovascular outcomes in patients with acute coronary syndrome and diabetes: Rationale, design, and baseline characteristics of the BETonMACE trial. *Am Heart J* 2019;217:72–83. [PubMed: 31520897]
22. Tamura RE, Ferreira De Vasconcellos J, Sarkar D, Libermann TA, Fisher PB, Zerbini LF. GADD45 Proteins: Central Players in Tumorigenesis

23. Kazazian K, Haffani Y, Ng D, et al. FAM46C/TENT5C functions as a tumor suppressor through inhibition of Plk4 activity. *Commun Biol* 2020;3(1). [PubMed: 31925311]
24. Plumb M, Marashi F, Green L, et al. Cell Cycle Regulation of Human Histone HI MRNA (Cloned Hi Gene/Gene Expression/Hybridization/Cell Proliferation) Vol 81.; 1984.
25. Michaelis KA, Knox AJ, Xu M, et al. Identification of growth arrest and DNA-damage- inducible gene β (GADD45 β) as a novel tumor suppressor in pituitary gonadotrope tumors. *Endocrinology* 2011;152(10):3603–3613. [PubMed: 21810943]
26. Lasorella A, Rothschild G, Yokota Y, Russell RG, Iavarone A. Id2 Mediates Tumor Initiation, Proliferation, and Angiogenesis in Rb Mutant Mice . *Mol Cell Biol* 2005;25(9):3563–3574. [PubMed: 15831462]
27. Ketchart W, Smith KM, Krupka T, et al. Inhibition of metastasis by HEXIM1 through effects on cell invasion and angiogenesis. *Oncogene* 2013;32(33):3829–3839. [PubMed: 22964639]
28. Marconcini L, Marchiò S C-Fos-Induced Growth Factorvascular Endothelial Growth Factor D Induces Angiogenesis in Vivo and in Vitro Vol 96.; 1999.
29. Christiansen VJ, Sims PJ, Hamilton KK. Complement C5b-9 increases plasminogen binding and activation on human endothelial cells. *Arterioscler Thromb Vasc Biol* 1997;17(1):164–171. [PubMed: 9012652]
30. Safford M, Collins S, Lutz MA, et al. Egr-2 and Egr-3 are negative regulators of T cell activation. *Nat Immunol* 2005;6(5):472–480. [PubMed: 15834410]
31. Colombo M, Galletti S, Garavelli S, et al. Notch signaling deregulation in multiple myeloma: A rational molecular target. *Oncotarget* 2015;6(29):26826–26840. [PubMed: 26308486]
32. Oommen KS, Newman AP. Co-regulation by Notch and Fos is required for cell fate specification of intermediate precursors during *C. elegans* uterine development. *Development* 2007;134(22):3999–4009. [PubMed: 17942488]
33. Boareto M, Iber D, Taylor V. Differential interactions between Notch and ID factors control neurogenesis by modulating Hes factor autoregulation. *Development* 2017;144(19):3465–3474. [PubMed: 28974640]
34. Nguyen D, Fayol O, Buisine N, Lecorre P, Uguen P. Functional interaction between HEXIM and Hedgehog signaling during *Drosophila* wing development. *PLoS One* 2016;11(5):e0155438. [PubMed: 27176767]
35. Zou Z, Ohta T, Miura F, Oki S. ChIP-Atlas 2021 update: a data-mining suite for exploring epigenomic landscapes by fully integrating ChIP-seq, ATAC-seq and Bisulfite-seq data. *Nucleic Acids Res* 2022;50(W1):W175–W182. [PubMed: 35325188]
36. Matys V, Kel-Margoulis OV., Fricke E, et al. TRANSFAC and its module TRANSCOMP: transcriptional gene regulation in eukaryotes. *Nucleic Acids Res* 2006;34(Database issue).
37. Morton T, Petricka J, Corcoran DL, et al. Paired-end analysis of transcription start sites in *Arabidopsis* reveals plant-specific promoter signatures. *Plant Cell* 2014;26(7):2746–2760. [PubMed: 25035402]
38. Khachigian LM, Lindner V, Williams AJ, Collins T. Egr-1-induced endothelial gene expression: a common theme in vascular injury. *Science* (1979) 1996;271(5254):1427–1431.
39. DeCicco-Skinner KL, Henry GH, Cataisson C, et al. Endothelial cell tube formation assay for the in vitro study of angiogenesis. *Journal of Visualized Experiments* 2014;(91).
40. Hoeben A, Landuyt B, Highley MS, Wildiers H, van Oosterom AT, de Bruijn EA. Vascular endothelial growth factor and angiogenesis. *Pharmacol Rev* 2004;56(4):549–580. [PubMed: 15602010]
41. Hamik A, Wang B, Jain MK. Transcriptional regulators of angiogenesis. *Arterioscler Thromb Vasc Biol* 2006;26(9):1936–1947. [PubMed: 16778118]
42. Brindle NPJ, Saharinen P, Alitalo K. Signaling and functions of angiopoietin-1 in vascular protection. *Circ Res* 2006;98(8):1014–1023. [PubMed: 16645151]
43. Jakobsson L, Franco CA, Bentley K, et al. Endothelial cells dynamically compete for the tip cell position during angiogenic sprouting. *Nat Cell Biol* 2010;12(10):943–953. [PubMed: 20871601]
44. Phng LK, Gerhardt H. Angiogenesis: a team effort coordinated by notch. *Dev Cell* 2009;16(2):196–208. [PubMed: 19217422]

45. Nosedá M, Chang L, McLean G, et al. Notch activation induces endothelial cell cycle arrest and participates in contact inhibition: role of p21Cip1 repression. *Mol Cell Biol* 2004;24(20):8813–8822. [PubMed: 15456857]
46. Siekmann AF, Lawson ND. Notch signalling limits angiogenic cell behaviour in developing zebrafish arteries. *Nature* 2007;445(7129):781–784. [PubMed: 17259972]
47. Liu H, Mei FC, Yang W, et al. Epac1 inhibition ameliorates pathological angiogenesis through coordinated activation of Notch and suppression of VEGF signaling. *Sci Adv* 2020;6(1):eaay3566. [PubMed: 31911948]
48. Sun Y, Liu CH, SanGiovanni JP, et al. Nuclear receptor ROR α regulates pathological retinal angiogenesis by modulating SOCS3-dependent inflammation. *Proc Natl Acad Sci U S A* 2015;112(33):10401–10406. [PubMed: 26243880]
49. Wang B, Zhang M, Takayama T, et al. BET Bromodomain Blockade Mitigates Intimal Hyperplasia in Rat Carotid Arteries. *EBioMedicine* 2015;2(11):1650–1661. [PubMed: 26870791]
50. Alexanian M, Przytycki PF, Micheletti R, et al. A transcriptional switch governs fibroblast activation in heart disease. *Nature* 2021;595(7867):438–443. [PubMed: 34163071]
51. Bhadury J, Nilsson LM, Muralidharan SV, et al. BET and HDAC inhibitors induce similar genes and biological effects and synergize to kill in Myc-induced murine lymphoma. *Proc Natl Acad Sci U S A* 2014;111(26):E2721–30. [PubMed: 24979794]
52. Latif AL, Newcombe A, Li S, et al. BRD4-mediated repression of p53 is a target for combination therapy in AML. *Nat Commun* 2021;12(1):241. [PubMed: 33431824]
53. Ding N, Hah N, Yu RT, et al. BRD4 is a novel therapeutic target for liver fibrosis. *Proc Natl Acad Sci U S A* 2015;112(51):15713–15718. [PubMed: 26644586]
54. Tian B, Zhao Y, Sun H, Zhang Y, Yang J, Brasier AR. BRD4 mediates NF-kappaB-dependent epithelial-mesenchymal transition and pulmonary fibrosis via transcriptional elongation. *Am J Physiol Lung Cell Mol Physiol* 2016;311(6):L1183–L1201. [PubMed: 27793799]
55. Li Z, Guo J, Wu Y, Zhou Q. The BET bromodomain inhibitor JQ1 activates HIV latency through antagonizing Brd4 inhibition of Tat-transactivation. *Nucleic Acids Res* 2013;41(1):277–287. [PubMed: 23087374]
56. Song S, Liu L, Yu Y, et al. Inhibition of BRD4 attenuates transverse aortic constriction- and TGF-beta-induced endothelial-mesenchymal transition and cardiac fibrosis. *J Mol Cell Cardiol* 2019;127:83–96. [PubMed: 30529267]
57. Bid HK, Kerk S. BET bromodomain inhibitor (JQ1) and tumor angiogenesis. *Oncoscience* 2016;3(11–12):316–317. [PubMed: 28105454]
58. Mohammed SA, Albiero M, Ambrosini Samuele E, et al. The BET protein inhibitor apabetalone rescues diabetes-induced impairment of angiogenic response by epigenetic regulation of thrombospondin-1. *Antioxid Redox Signal* 2022;36(10–12):667–684. [PubMed: 34913726]
59. Chavkin NW, Genet G, Poulet M, et al. Endothelial cell cycle state determines propensity for arterial-venous fate. *Nat Commun* 2022;13(1):5891. [PubMed: 36202789]
60. Nosedá M, Niessen K, McLean G, Chang L, Karsan A. Notch-dependent cell cycle arrest is associated with downregulation of minichromosome maintenance proteins. *Circ Res* 2005;97(2):102–104. [PubMed: 15976316]
61. Pitulescu ME, Schmidt I, Giaimo BD, et al. Dll4 and Notch signalling couples sprouting angiogenesis and artery formation. *Nat Cell Biol* 2017;19(8):915–927. [PubMed: 28714968]
62. Lamalice L, le Boeuf F, Huot J. Endothelial cell migration during angiogenesis. *Circ Res* 2007;100(6):782–794. [PubMed: 17395884]
63. Wei Y, Gong J, Thimmulappa RK, Kosmider B, Biswal S, Duh EJ. Nrf2 acts cell-autonomously in endothelium to regulate tip cell formation and vascular branching. *Proc Natl Acad Sci U S A* 2013;110(41):E3910–8. [PubMed: 24062466]
64. Ryan TE, Yamaguchi DJ, Schmidt CA, et al. Extensive skeletal muscle cell mitochondriopathy distinguishes critical limb ischemia patients from claudicants. *JCI Insight* 2018;3(21).
65. Yan T, Liang J, Gao J, et al. FAM222A encodes a protein which accumulates in plaques in Alzheimer's disease. *Nat Commun* 2020;11(1):411. Highlights [PubMed: 31964863]

Highlights

- Despite most reports focusing on BET epigenetic reader proteins BRD2, BRD3, BRD4 in controlling pathogenic gene expression, as supported by BET inhibitors decreasing endothelial inflammation, atherosclerosis, and pulmonary hypertension, BETs also direct the basal endothelial cell (EC) transcriptome, as defined here in RNA-Seq data from ECs under basal conditions in the absence versus presence of the specific pan-BET inhibitor JQ1.
- The BET-regulated endothelial transcriptional program under basal conditions includes genes involved in core aspects of endothelial biology as well as a subset of mRNAs whose basal expression is increased significantly after BET inhibition (BET inhibitors, siBRD4).
- Analysis of BET-regulated mRNAs in ECs under basal conditions identifies Chromosome 12 Open Reading Frame 34 (C12orf34), also known as Family with Sequence Similarity 222 Member A (FAM222A), as a unique, basally-expressed, BET-regulated gene in ECs with no previously identified role in endothelial biology; data presented here demonstrates FAM222A is essential for EC migration, proliferation, vascular sprouting and angiogenic responses *in vitro* and *ex vivo* by modulating expression of key VEGF and NOTCH pathway mediators. Silencing FAM222A *in vivo* impairs angiogenesis in the neonatal oxygen induced retinal (OIR) neovascularization model, with similar effects on key VEGF and NOTCH mediators.

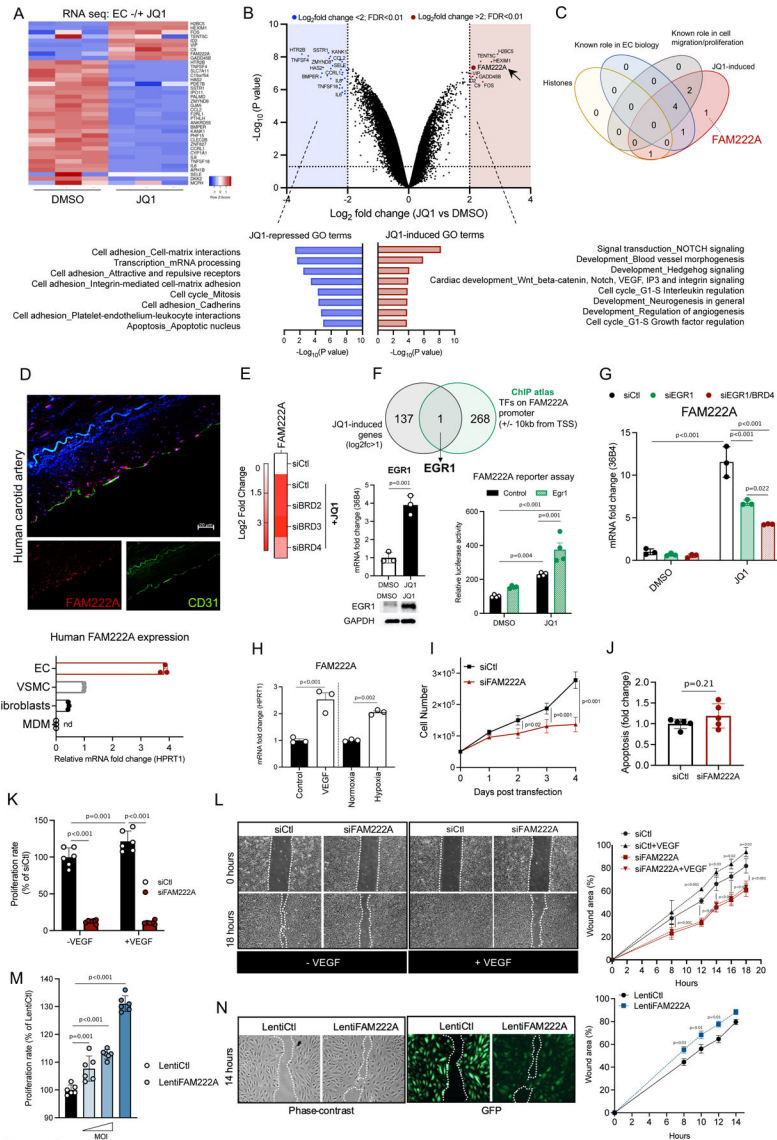


Figure 1

Figure 1: BETs regulate the basal endothelial transcriptome, including FAM222A - an essential, novel determinant of EC proliferation and migration.

Human umbilical vein endothelial cells (HUVEC) under basal conditions were treated with vehicle control (DMSO) or the highly specific BET inhibitor JQ1 (500nM, here and throughout, unless otherwise specified, 3 hours) before performing genome-wide RNA-seq analysis². **A.** Heatmap of EC genes under basal conditions whose mRNA was significantly repressed or induced by JQ1 (log2 fold change, >2 or <2 vs control, here and throughout; FDR, <0.05) is shown. Color indicates z-score normalized expression from +2.5 (red) to -2.5 (blue). **B. Upper:** Volcano plot of significantly JQ1-induced (red) or -repressed (blue) mRNA levels (vs control, log2 fold change, < or >2; FDR, <0.05). **Lower:** GO pathway analysis of mRNAs significantly modulated by JQ1, organized by adjusted log10 p-value. **C.** Venn diagram of the top 9 genes whose mRNA was most induced by JQ1; FAM222A was the only non-histone, JQ1-induced gene with no reported role in EC or cell cycling/proliferation. **D. Upper:** Representative immunofluorescent staining in normal

human carotid artery for FAM222A (red), CD31 (green) and nuclei (DAPI, blue). Scale bar; 20 μ m. **Lower:** Relative FAM222A mRNA expression in HUVECs, primary vascular smooth muscle cells (VSMCs, coronary artery), fibroblasts (skin), and monocyte-derived macrophages (MDMs, peripheral blood) (n=3 for all cell types, ND = non-detected, here and throughout), normalized to VSMCs. **E.** Heatmap displaying relative FAM222A mRNA expression in HUVECs after siBRD2, siBRD3, siBRD4 or siControl (siCTL, all 50 nM) transfection, either alone or with concurrent JQ1 treatment (3 hours, 500nM, n=3 per group). **F. Upper:** Overlap analysis of significantly JQ1-induced genes (log₂ fold change>1, n = 127) in ECs and transcription factors predicted to bind to the FAM222A promoter (+/- 10kb from TSS, n = 268, CHIP Atlas³⁵) identifies EGR1 as the sole gene meeting both criteria in these datasets (Venn diagram). **Lower left:** EGR1 mRNA and protein expression after JQ1 treatment (3 hours, n = 3 per group). **Lower right:** Relative luciferase activity of the human FAM222A promoter (1523 bp proximal to TSS) in human embryonic kidney (HEK) 293T cells transfected with EGR1 overexpression vector in the presence or absence of JQ1 (3 hours, n = 4 per group). **G.** Relative FAM222A mRNA expression in HUVECs after siEGR1 alone or with siBRD4 co-transfection in the presence of JQ1 or its absence (DMSO) (3 hours, n=3 per group). **H.** FAM222A mRNA expression in HUVECs stimulated by VEGF (50ng/ml) or hypoxia (O₂ 1%, 3 hours for both, n=3 per group). **I.** Cell number assessed in HUVEC 4 days after transfection with siFAM222A or siCtl (both 50nM, n=3 per group). **J.** Apoptosis assessed using caspase 3/7 activation in siFAM222A- or siCtl-transfected ECs (24 hrs, n=5 per group). **K.** Cell proliferation was measured using BrdU incorporation without or with VEGF stimulation (50ng/ml, n=6 per group). **L.** EC migration after siFAM222A or siCtl transfection as measured by scratch wound assay, without or with VEGF stimulation (50ng/ml, 18 hours). Representative images (left) and quantification of wound closure (right) shown. Bar scale: 50 μ m (n=3 per group). **M.** HUVECs were transfected with validated FAM222A overexpression (LentiFAM222A) or Control (LentiCtl) GFP-expressing lentivirus prior to performing BrdU cell proliferation assays as before. FAM222A-overexpressing ECs were transfected at different multiplicity of infection (MOI) of the respective vector determine before assessing cell proliferation (n= 6 per group). **N.** EC migration was assessed by wound closure assay as before. Representative phase-contrast and fluorescent images of GFP-positive cells (left) and quantification of wound closure over time (right) are shown. Scale bar; 100 μ m (n=3 per group, 14 hrs). Each data point represents a biological replicate. Data presented as mean \pm SEM throughout. P values by one-way ANOVA with Tukey post-test except for Student's test in F (lower left) and J,.

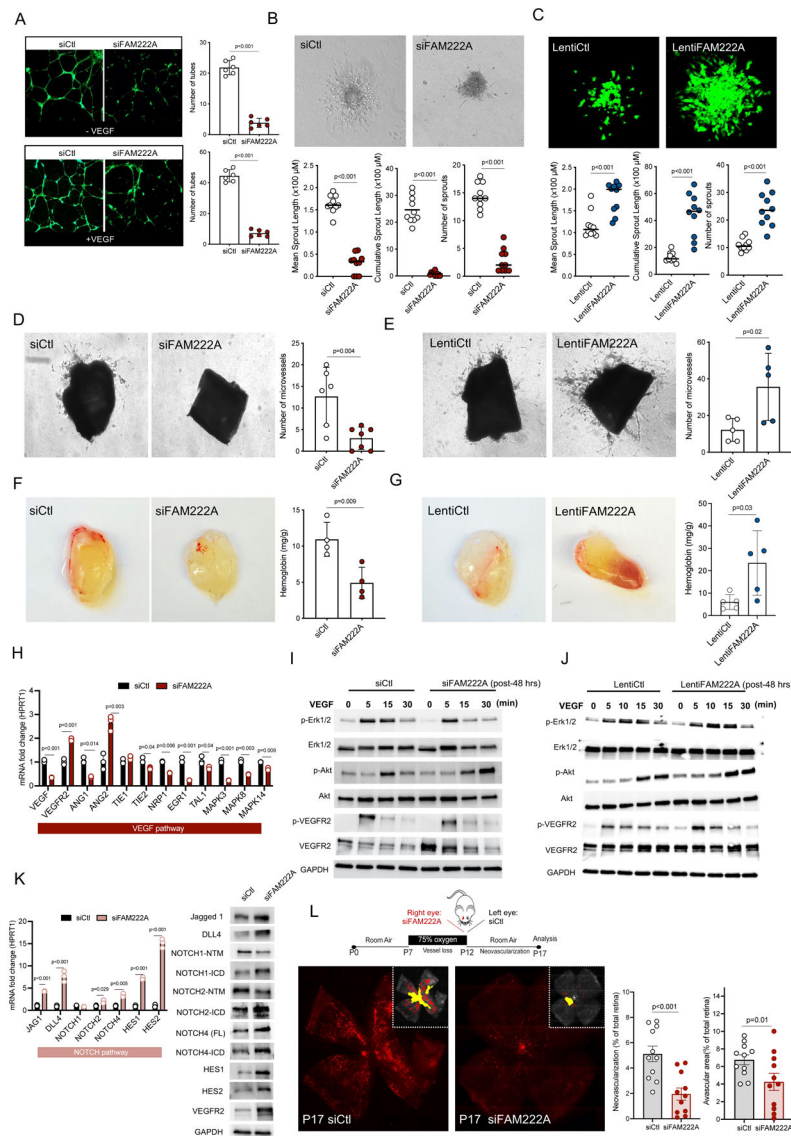


Figure 2

Figure 2: FAM222A regulates EC network formation, sprouting, angiogenic mediator expression and angiogenesis in a coordinated manner *in vitro*, *ex vivo*, and *in vivo*.

A. Network tube formation assays in Matrigel were performed in ECs transfected with siFAM222A or siCtl in the absence (upper) or presence (lower) of VEGF (50ng/ml). Representative images of Calcein-labeled tubes (left) and tube number quantification (right) are shown. Scale bar; 100μm (n=6 per group). **B. Endothelial spheroid sprouting assays** were performed after FAM222A silencing (siFAM222A) or control (siCtl) transfection. **C.** Representative fluorescent images (upper) and quantification (lower, n = 10 per group) of mean sprout length, cumulative sprout number, and sprouts per spheroid after overexpression of FAM222A (LentiFAM222A) or control vectors (LentiCtl) in ECs after VEGF stimulation (50ng/ml). Representative images (upper) and quantification (lower) of mean sprout length, cumulative sprout number, and sprouts per spheroid are shown. Scale bar; 100μm. **Microvessel sprouting in *ex vivo* aortic ring assays** of **D.** siFAM222A (vs siCtl) and **E.** lentiFAM222A (vsLentiCtl) treated mouse aortic rings

embedded in Matrigel (10 days post transfection/infection). Representative images (left) and quantification (right) of microvessel number per ring are shown. Scale bar; 100 μ m (n=5–7 per group). **Matrigel vascularization assays *in vivo*** using plugs mixed with HUVECs treated with **F.** siFAM222A (vs siCtl) or **G.** LentiFAM222A/LentiCtl before injection into the flank region of wild type mice were performed. Representative images (left) and Matrigel vascularization, using Hemoglobin (Hb) content (normalized to plug weight) 7 days post implantation (right) are shown (n= 4–5 per group). **H.** siFAM222A or siCtl-transfected ECs underwent VEGF-stimulation (50ng/ml, 48 hrs) before measuring mRNA levels of the VEGF-regulated genes shown (n=3 per group). **I.** As in (H), after 48 hrs, siFAM222A- or siCtl-transfected ECs underwent VEGF stimulation prior to immunoblotting for total and phosphorylated Erk1/2, Akt and VEGFR2 at the time points shown. **J.** VEGF-stimulated phosphorylation assays as in (I) were repeated in ECs overexpressing FAM222A (LentiFAM222A) or control (LentiCtl) constructs prior to immunoblotting for total and phosphorylated Erk1/2, Akt and VEGFR2 at the time points shown. **K.** NOTCH pathway gene mRNA levels (left) and protein (right) levels were measured in siFAM222A or siCtl-transfected ECs 48 hrs after VEGF-stimulation as above (H, I)(n=3 per group). **L. Upper:** Schematic diagram of the mouse neonatal oxygen-induced hyperoxia (OIR) model. At P7, pups of both sexes (sex determination being imprecise at this age) and their nursing mothers were exposed to hyperoxia (75% oxygen, 5 consecutive days, vessel loss phase). Upon return to room air (P12), pups underwent intravitreal injection with FAM222A or Control siRNAs (2 μ g) before sacrifice at P17 (neovascularization phase). **Lower: Left** - Representative retinal flat mount images after staining for retinal vasculature (isolectin B4) from neonatal pups injected at P17 with siCtl or siFAM222A. The avascular (yellow) and neovascularization (red) areas are shown. **Right** - Quantification of avascular and neovascularization areas as a percentage of total retina (n=11 per group). Each data point represents an individual mouse or biological replicate. In all cases, data are presented as mean \pm SEM. P values by Student's test.